The reductive deposition of quaternary pyridinium corrosion inhibitor multilayers on glassy carbon electrodes[1]

Rick P.C. Wong, Jennifer E. Wong, and Viola I. Birss

Abstract: The redox behaviour of several quaternary pyridinium corrosion inhibitors ("Quats") at glassy carbon (GC) electrodes has been investigated in neutral aqueous solutions. The primary emphasis is on *n*-butyl-3-(*N*-octylcarbamyl)pyridinium bromide, one of the Quats determined to have very good corrosion inhibition properties based on parallel weight loss experiments. It is demonstrated that the reduction of the Quats, which occurs in a two-electron reaction at potentials negative of –1.0 V vs. SSCE, results in the formation of a neutral product. This forms a porous film on the electrode surface, with clusters that expand and thicken as more Quat deposits, as confirmed by atomic force microscopy. The film charge density reaches a maximum of ~4 mC/cm^2, equivalent to more than 100 monolayers of Quat, after which no further Quat can be deposited, suggesting full surface coverage by a nonconducting product. The Quat multilayer can then be redissolved at potentials positive of ~ –0.2 V, during its oxidation back to its original solution-soluble form.

Key words: quaternarized pyridinium compounds, reductive film deposition, glassy carbon, multilayer, corrosion inhibitors, cyclic voltammetry, AFM.

Résumé : Opérant dans des solutions aqueuses neutres, on a étudié le comportement redox, au niveau d'électrodes de carbone vitreux (CV), de plusieurs sels de pyridinium quaternaires, des inhibiteurs de la corrosion (« Quats »). L'accent a principalement été mis sur le bromure de *n*-butyl-3-(*N*-octylcarbamyl)pyridinium, un des quatre Quats qui, sur la base d'expériences parallèles de pertes de poids, devrait présenter de très bonnes propriétés d'inhibition de la corrosion. Il a été démontré que la réduction du Quats, une réaction à deux électrons à des potentiels négatifs de –1,0 V vs. SSCE, conduit à la formation d'un produit neutre. Tel que confirmé par une microscopie de forces atomiques, celui-ci forme un film poreux sur la surface de l'électrode, avec des agrégats qui conduisent à une expansion et un épaississement avec les dépôts additionnels de Quats. La densité de charge du film atteint un maximum de ~4 mC/cm^2, équivalent à plus de 100 monocouches de Quat, après quoi il ne peut plus se déposer de Quat, ce qui suggère que la surface totale est couverte par un produit qui ne conduit pas l'électricité. La multicouche de Quat peut alors être redissoute à des potentiels positifs de ~ –0.2 V, durant sa réoxydation à sa forme originale soluble dans la solution.

Mots clés : dérivés pyridinium quaternaires, dépôt d'un film de réduction, carbone vitreux, multicouche, inhibiteurs de corrosion, voltampérométrie cyclique, AFM.

[Traduit par la Rédaction]

Introduction

Quaternary pyridinium compounds ("Quats", Fig. 1*a*) are a class of cationic organic corrosion inhibitors used for the protection of metals such as carbon steel in pipeline and drilling equipment. These inhibitors are relatively low in cost and are especially effective in environments that contain brine and high concentrations of H_2S or CO_2. While the mechanism of the corrosion protection of metals by Quats remains essentially unknown, it has been surmised that Quats adsorb strongly, thus blocking local anodic and cathodic surface sites.

We have recently examined (1)[3,4] the impact of the addition of Quats to aqueous neutral and weakly alkaline solutions on Pt electrochemistry. It was demonstrated that Pt oxide formation and reduction, as well as hydrogen adsorption and evolution, could be essentially fully suppressed by the presence of certain Quats in solution, at concentrations >40 μmol/L (1). Quats that showed a high propensity for adsorption on Pt also served to protect carbon steel from corro-

Received 7 June 2004. Published on the NRC Research Press Web site at http://canjchem.nrc.ca on 3 December 2004.

R.P.C. Wong, J.E. Wong, and V.I. Birss.[2] Department of Chemistry, University of Calgary, 2500 University Drive N.W., Calgary, AB T2N 1N4, Canada.

[1]This article is part of a Special Issue dedicated to the memory of Professor Don Irish.
[2]Corresponding author (e-mail: birss@ucalgary.ca).
[3]J.E. Wong, D.T. Cramb, and V.I. Birss. Article in preparation.
[4]J.E. Wong, D.T. Cramb, and V.I. Birss. Article in preparation.

 doi: 10.1139/V04-127

Fig. 1. (*a*) Generic structure of quaternary pyridinium compounds (Quats) and structures of (*b*) *n*-butyl-3-[hydroxy(octylamino)methyl] pyridinium bromide (Quat 1); (*c*) *n*-butyl-3-(*N*-octylcarbamyl)pyridinium bromide (Quat 2); (*d*) *n*-benzyl-3,5-dimethyl pyridinium bromide (Quat 3); (*e*) *n*-decyl-3-(*N*-hexylcarbamyl) pyridinium bromide (Quat 4).

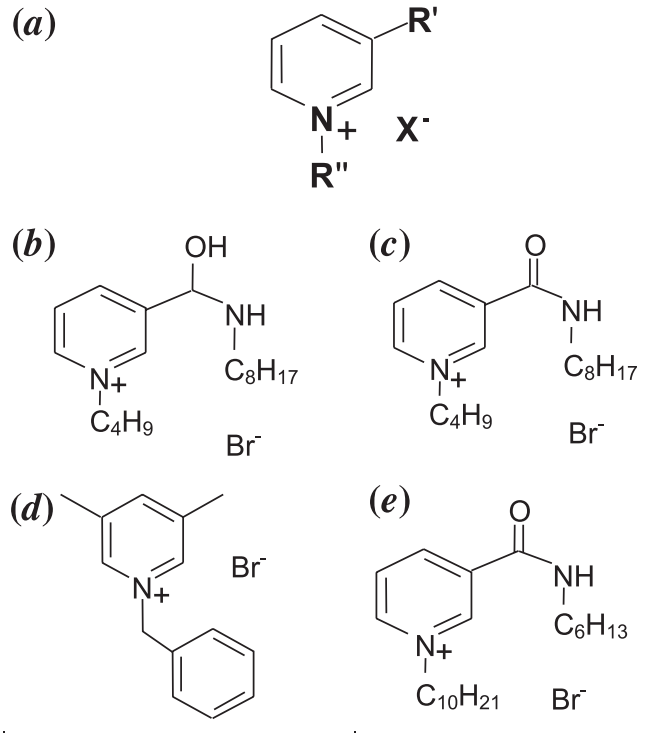

sion in parallel tests in brine solutions. It was generally observed (1) that Quats containing alkyl chains of C-8 or longer, either in the meta position or attached to the pyridinium nitrogen (Fig. 1*a*), were most effective in decreasing the corrosion rate of carbon steel. Corresponding quartz crystal microbalance (QCMB) results (1) showed a mass increase equivalent to about two monolayers of adsorbed molecules in these experiments. It was also shown that (1), once Pt electrochemistry was blocked by Quat adsorption, the normal potential window could be widened well beyond the normal limit defined by hydrogen evolution, allowing potentials to be reached at which the Quats can be reduced. This led to the deposition of a Quat multilayer.

The reduction of related compounds (e.g., 4-cyano-1-methyl pyridinium) has been reported previously, and it has been suggested that they can be reductively dimerized, forming the viologen form of the compound (2). Nicotinamide, another compound with a closely related structure, has also been shown to reduce electrochemically (3–5), forming a neutral hydropyridine monomer or dimer, while dimerization is proposed during reduction in acidic environments. 2-Vinyl pyridine has also been shown to reduce on a steel electrode (6), possibly forming a polymeric surface product.

In the present work, the behavior of Quats at a stable electrode surface, not susceptible to dissolution, was examined using a combination of cyclic voltammetry and constant potential methods, as well as atomic force microscopy (AFM). Glassy carbon (GC) was chosen for this purpose, primarily because of its high overpotential for hydrogen evolution, allowing easy access to negative potentials. Also, GC electrodes are not readily oxidized and display only minimal surface electrochemistry.

In this paper, the primary focus is on the electrochemical behavior of a specific Quat, namely *n*-butyl-3-(*N*-octylcarbamyl)pyridinium bromide (Quat 2, Fig. 1*c*), chosen because of the high degree of protection it offers carbon steel from corrosion in weight loss experiments in brine solutions (7). A pure form of this Quat was synthesized to avoid the impurities commonly encountered in the commercial Quat mixtures. Three other Quats (Quats 1, 3, and 4, Figs. 1*b*–1*e*) were also examined for comparison purposes. Cyclic voltammetric studies show that all of the Quats (8) can be reduced, resulting in the deposition of a Quat multilayer on the GC surface. The properties of this layer and its impact on the corrosion inhibition properties of Quats will also be discussed.

Experimental methods

Electrodes and surface preparation

The working electrode consisted of an 11 mm diameter glassy carbon (GC) rod, electrically connected to a copper wire using conducting silver epoxy (Allied Electronics, 2400 Circuit Works). To ensure a high quality connection and good adhesion, a layer of standard epoxy was applied on top of the conducting silver epoxy. The GC rod was then imbedded in an inert resin (Scandia, 58 Hagen), exposing only its cross-sectional end (0.95 cm^2). All current and charge densities in this paper are calculated on the basis of this apparent electrode area.

Prior to use, the GC electrode was hand-polished on a flat surface using 600 grit silicon carbide emery paper. The electrode was then polished using a coarse suspension of alumina (Metaserv, 7.0 μm) on a Rayfinal polishing cloth (Micro-Metallurgical Ltd.). Progressively finer alumina powder (E.T. Enterprises, 1.0, 0.3, and 0.05 μm) was then used, until a mirror-like surface was obtained (9, 10). The polished electrode was then cleaned with triply distilled water in an ultrasonic bath for at least 10 min to remove any alumina powder left on the surface.

The counter electrode (CE) was a large surface area Pt gauze electrode, embedded in soft glass tubing. A saturated sodium calomel electrode (SSCE, 0.235 V vs. SHE) was used as the reference electrode (RE) and all potentials are referred to the SSCE in this paper.

Instrumentation, cells, and solutions

All CV measurements were performed using an EG&G PARC 273 potentiostat/galvanostat and all data were recorded on a Hewlett-Packard 7045B X-Y recorder. A two-compartment electrochemical cell was employed, with the RE in one compartment joined to the main compartment containing the WE and CE, via a Luggin capillary. The GC electrode was suspended face-downwards in this cell configuration. Nitrogen bubbling, either through or above the cell solution, served to deaerate the cell solutions.

Water was triply distilled using a Corning Mega-Pure-6A system. A 0.05 mol/L KH_2PO_4 + 0.03 mol/L NaOH pH 7.2 phosphate buffer solution was prepared according to the CRC Handbook (11). All reagents were Fisher Certified or

ACS grade and were used as received. The temperature of the solutions ranged from 20 to 22 °C. Quaternary pyridinium compounds (Quats) were provided by Brenntag Canada (formerly Travis Chemicals), either in solution or in crystalline form, and their general structure is presented in Fig. 1*a*. The primary emphasis of this paper is on the *n*-butyl-3-(*N*-octylcarbamyl)pyridinium bromide (Quat 2), as shown in Fig. 1*c*, but *n*-butyl-3-[hydroxy(octylamino)methyl] pyridinium bromide (Quat 1, Fig. 1*b*), *n*-benzyl-3,5-dimethyl pyridinium bromide (Quat 3, Fig. 1*d*), and *n*-decyl-3-(*N*-hexylcarbamyl) pyridinium bromide (Quat 4, Fig. 1*e*) were also investigated. Stock solutions of these Quats of 100 mmol/L were used in this work.

Atomic force microscopy (AFM)

Samples were prepared using a lithographically deposited (for ease of positioning of the AFM tip) Pt sputtered coated glass working electrode (apparent area 0.75 cm^2), cleaned electrochemically in stirred, deaerated 1 mol/L H_2SO_4 until a steady-state CV was observed. The potential was then cycled between –0.6 and 1.0 V vs. SSCE in a stirred, deaerated pH 7.2 phosphate buffer solution. An aliquot of the 100 mmol/L Quat stock solution was added such that the final solution concentration was 0.25 mmol/L and after a period of potential cycling, the potential was held at –0.9 V to deposit the Quat multilayer. The electrode was then rinsed, allowed to air-dry, and imaged using a Molecular Imaging, Inc. Nanoscope II instrument in MacMode in air. The cantilever used had a force constant ranging from 2 to 5 N/m.

Results and discussion

General electrochemical behaviour of Quats at GC in neutral phosphate buffer solutions

After 30 min of cycling in a pH 7.2 phosphate buffer solution in the range of –1.5 to 1.0 V vs. SSCE, the bare, polished GC electrode reveals an almost featureless cyclic voltammetric (CV) response (Fig. 2*a*), as previously reported in the literature (12–17). Only capacitive current is seen over the entire potential range from –1.5 to 1.0 V, with no evidence for the onset of the HER until potentials below –1.2 V.

Upon the addition of an aliquot (2 mmol/L in cell) of *n*-butyl-3-(*N*-octylcarbamyl)pyridinium bromide (Quat 2) to the phosphate buffer solution, the magnitude of the charging current does not change significantly, suggesting that Quat 2 does not adsorb on the GC surface (Fig. 2*a*). However, at more negative potentials, an obvious set of redox peaks (A_1 and C_1) are seen. Notably, these features are quite similar to those observed at Pt (1), although the anodic peak potential is more positive on Pt (0.3 V) than on GC (0.1 V) under otherwise the same conditions. Also, previous work on Pt in pH 7.2 phosphate buffer demonstrated that the Quat reduction peak was sometimes difficult to resolve from the currents because of hydrogen evolution, which is the main reason that GC electrodes were chosen for the present work.

In the case of the addition of Quats 1 and 3 to the phosphate buffer solution, Figs. 2*b* and 2*c*, respectively, show very similar results, except that the anodic peak A_1 is actually composed of two peaks in the first few cycles of potential. The origin of these two anodic peaks is still unclear.

Fig. 2. (*a*) CV of GC in deaerated pH 7.2 phosphate buffer solution at 100 mV/s, before (—) and after (----) the addition of 2 mmol/L Quat 2. Inset: CV response of GC before (—) and after (····) the addition of 1.6 mmol/L KBr. (*b*) CV of GC in deaerated pH 7.2 phosphate buffer solution at 100 mV/s before (– – – –) and after the addition of 0.32 mmol/L (—) and 1.6 mmol/L (···) Quat 1. (*c*) CV of GC in deaerated pH 7.2 phosphate buffer solution at 100 mV/s before (– – – –) and after (—) the addition of 0.32 mmol/L Quat 3.

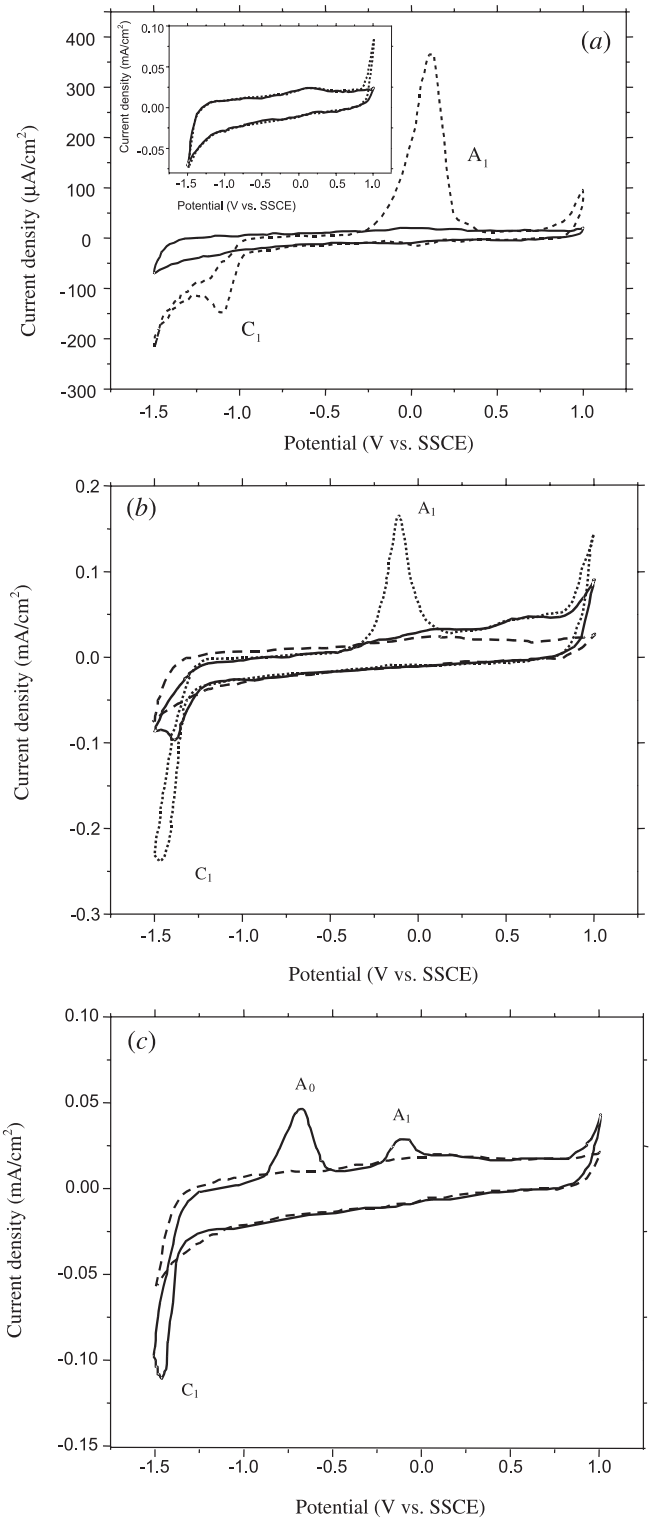

Scheme 1. Proposed redox mechanism of a typical Quat monomer.

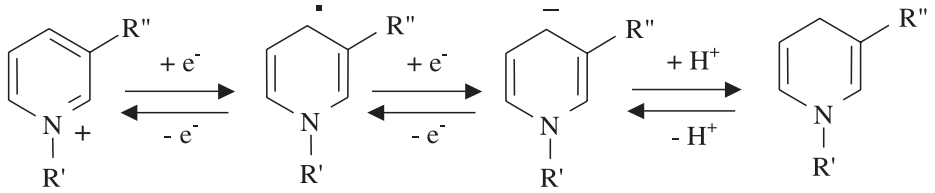

However, based on the discussion below, it is possible that the two anodic peaks often observed for the Quats reflects the stabilization of the one-electron oxidation product (Scheme 1), such that the transfer of each of the electrons is seen in a separate peak. Notably, their appearance separately seems to be related to the cycling time (exposure time) and the scan rate employed. Also, the size of the two anodic peaks decreases slightly and their potential shifts positively with increased time of cycling. Earlier published work with similar compounds, employing the dropping mercury electrode, showed two peaks during the reduction step, an example being the work of Carelli and Cardinali (2) for 4-cyano-1-methyl pyridinium in aqueous solutions of varying pH. Galvin and co-workers (4, 5) also observed two peaks during the reduction of nicotinamide under similar conditions and attributed the first reduction peak to the dimerization of the pyridinium rings, while the second peak was considered to be due to the reduction of the radical to form a neutral hydropyridine monomer.

The anodic current observed at potentials greater than ca. 0.85 V vs. SSCE, after the addition of the Quats to the cell solution (Fig. 2*a*), is due to the oxidation of bromide ions (rxn. [1]) (17), as was confirmed by the addition of 2 mmol/L KBr alone to the buffer solution (Fig. 2 inset).

[1] $2Br^- \rightarrow Br_2(aq) + 2e^-$

$E^0 = 0.863$ V (vs. SSCE)

To study Quat redox chemistry further, the lower potential limit (E_-) was changed from –1.5 V vs. SSCE to a less negative value of –1.0 V, as shown in Fig. 3 for Quat 2 (curve a). Both the C_1 and A_1 peaks have now disappeared, confirming that these peaks are coupled and that it is essential to first reduce the Quat to then allow its reoxidation. In another experiment, E_+ was lowered to –0.2 V, to prevent the oxidation process, while retaining an E_- of –1.5 V. The size of the C_1 peak decreases with each cycle of potential, as shown in Fig. 3 (curve b). The currents owing to double layer charging, between the A_1 and C_1 peaks, also then decrease with each cycle. Both of these results indicate that the C_1 peak reflects the deposition of a product on the electrode surface. Hence, when the potential is maintained negative of the A_1 peak, more Quat can be deposited on the GC surface with time. This appears to serve to increasingly block the electrode surface, reducing the activity of the surface towards further Quat reduction and also decreasing the capacitance of the double layer.

When E_+ was then increased back to its original value (from –0.2 to 1.0 V), a very large anodic peak was seen in the next anodic cycle, as shown in Fig. 3 (curve c). The potential of the A_1 peak is also shifted positively, implying that a more resistive (e.g., thicker) surface layer is now present.

Fig. 3. Effect of potential limits on CV response of GC electrode in 2 mmol/L Quat 2 in deaerated pH 7.2 phosphate buffer solution at 100 mV/s: steady-state response for $E_+ = 1.0$ V and $E_- = -1.0$ V, curve a (—); fifth cycle for $E_+ = -0.2$ V and $E_- = -1.5$ V, curve b (– – – –); first cycle with $E_+ = 1.0$ V and $E_- = -1.5$ V, curve c (·····).

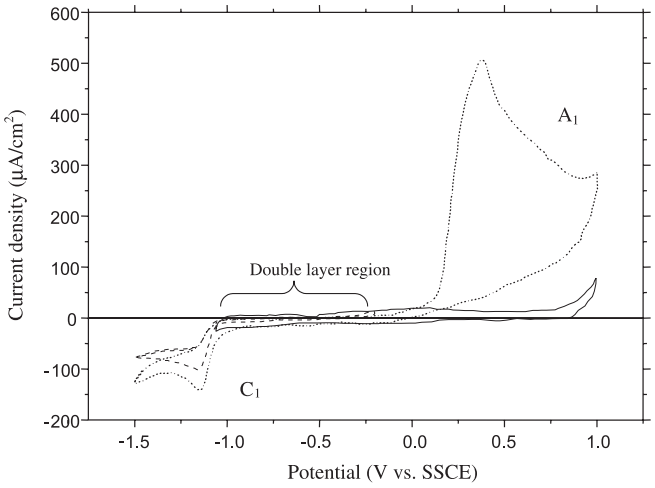

This likely indicates that the surface product, formed at negative potentials, is not very conductive. The reappearance of both redox peaks after extension of the potential limits beyond both the A_1 and C_1 peaks shows clearly that the A_1 peak depicts the removal of the surface product, allowing more Quat to be reduced and deposited in the following cathodic scan.

As a final confirmation of the deposition of a surface film in peak C_1, the GC electrode was removed from the Quat containing solution at $E_- = -1.5$ V, rinsed and blotted carefully with a tissue to remove any adhering solution, and then placed in a fresh phosphate buffer solution (without any added Quat). When the potential of this electrode was scanned positively from –1.5 V, the A_1 peak was clearly observed. However, the C_1 peak at –1.0 V was not seen in the following cathodic scan, and only a very small A_1 peak was seen in the next few anodic cycles. These results show clearly that the deposition of a reduced surface film occurs at negative potentials in the Quat-containing solution, and that it is oxidized and concurrently lost from the surface in the A_1 peak.

Overall, the results of Figs. 2 and 3 confirm that the Quats can be reduced at potentials negative of ca. –1.0 V, forming a surface product. However, this material is not oxidized at the GC electrode until a potential of ca. –0.3 V is reached. These electrochemical characteristics, seen for all of the Quats studied here, are very similar to those reported previously for NADH (3–5, 18), as discussed above (16). It

Fig. 4. Anodic peak (A_1) charge density as a function of Quat 2 concentration in stirred, deaerated pH 7.2 phosphate buffer solution after scanning negatively to –1.5 V at 100 mV/s. Inset: cathodic peak (C_1) charge density as a function of Quat 2 concentration in deaerated pH 7.2 phosphate buffer solution after scanning negatively to –1.5 V at 100 mV/s.

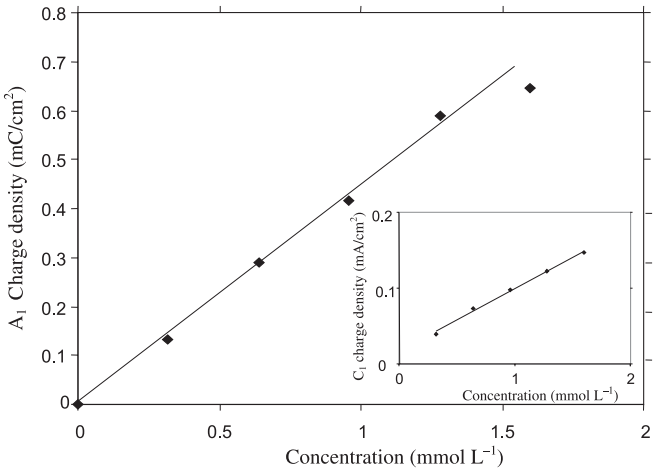

should be noted that the formation of a poorly conducting surface product at relatively negative potentials may be related to the corrosion inhibiting nature of the Quats at carbon steel electrodes, at which the corrosion potential can be quite negative at neutral pH.

Kinetics of Quat deposition

To determine the dependence of the Quat multilayer formation rate on Quat concentration, different volumes of the Quat stock solutions were added to the cell solution during continuous potential cycling, all at 100 mV s^{-1}. The CVs were recorded after a steady state was reached ~2 min after each addition. Figure 4 shows that the A_1 and A_2 (Fig. 4, inset) peak charge densities are linearly dependent on the Quat 2 concentration in the phosphate buffer solution. The results of Fig. 4 suggest that the rate of the C_1 deposition process, and hence, also of the A_1 oxidation reaction, is controlled by the rate of diffusion of Quat 2 to the electrode surface.

It is notable that the peak currents also increased significantly in size with solution stirring, consistent with this hypothesis. To test this further, the effect of the scan rate on the peak currents was examined. The zero current baseline for the C_1 peak was estimated consistently at each scan rate, assuming that the rate of the HER would be the same in each experiment. The results reveal that the C_1 peak current density exhibits a square root dependence on the scan rate, as shown in Fig. 5, again indicative of the control of Quat 2 reduction and deposition (peak C_1) rate by the transport of the Quat from solution to the electrode. Similar results were seen with Quats 1, 3, and 4, and also for Quats 1 and 2 at Pt.

Characteristics of Quat film at GC electrodes

The effect of holding the potential for various periods of time at –1.5 V in the presence of 4 mmol/L Quat 1 in the pH 7.2 phosphate buffer solution (stirred) was then examined. The results showed that the A_1 peak in the following anodic scan initially increased in size, at a rate proportional

Fig. 5. Dependence of the C_1 peak current density on the square rate of the sweep rate for 2 mmol/L Quat 2 in deaerated pH 7.2 phosphate buffer solution.

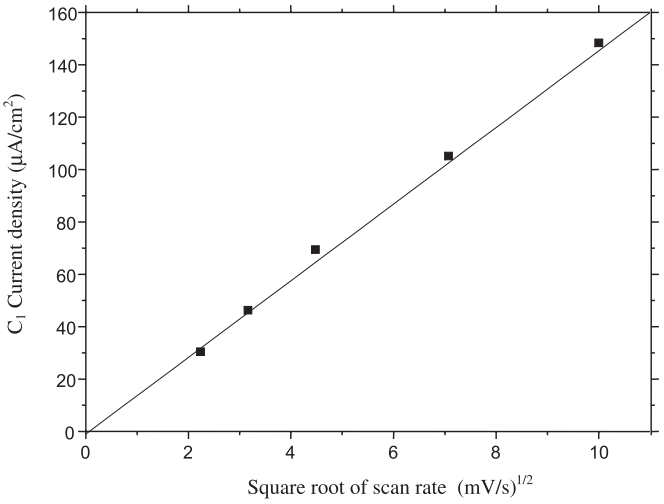

Fig. 6. Charge density of A_1 peak at GC as a function of holding time at –1.5 V vs. SSCE for 4 mmol/L Quat 2 in deaerated pH 7.2 phosphate buffer solution (100 mV/s).

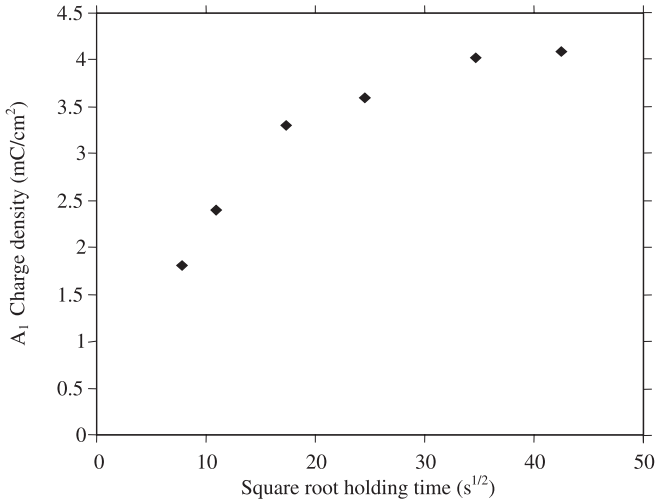

to the square root of the holding time. As shown in Fig. 6, the A_1 charge density appears to reach a threshold value of ca. 4 mC/cm^2 after about 30–40 min under these conditions (note that the dependence of the amount of deposited Quat is linear with the square root of holding time at earlier times, again indicative of diffusion-controlled Quat film deposition). In our earlier work with Pt substrates (1), the highest charge densities seen during Quat 2 deposition (at constant potential) and subsequent stripping at 2 mV/s were in the range of 2 to 5 mC/cm^2.

A parallel set of experiments in the 4 mmol/L Quat 1 solution, aimed at reaching an upper limit to the amount of Quat deposited by sweeping more slowly through the –1.5 to 1.0 V range, was then carried out. Figure 7 shows that the charge increases at slower sweep rates, which is expected if the rate of Quat deposition is diffusion controlled. At 5 mV/s, a charge of ca. 3 mC/cm^2 is seen, and it appears that

Fig. 7. Anodic vs. cathodic charge density obtained from 4 mmol/L Quat 2 in deaerated pH 7.2 phosphate buffer solution at different scan rates.

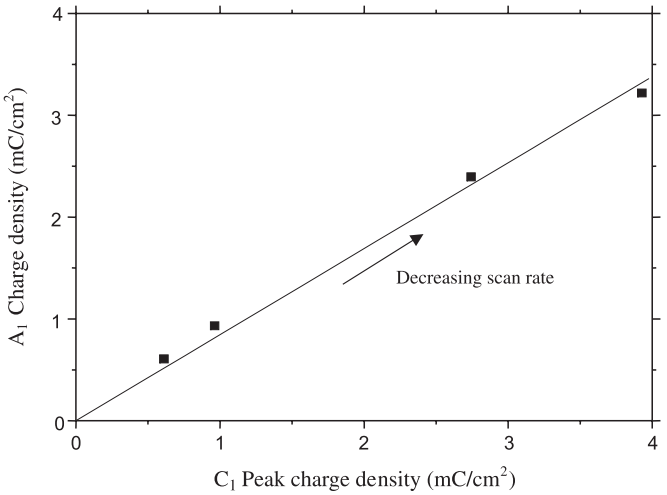

the plot would taper off at a somewhat higher charge density. Figure 7 also shows that the anodic and cathodic charges are very similar, especially at high scan rates, confirming that essentially all of the reduced product can be reoxidized under these conditions and also that the current baselines beneath the C_1 and A_1 peaks are being appropriately selected.

It is also possible that, as more Quat is deposited (higher concentrations, slower reduction sweep rates), not all of it is fully removed in the anodic scan. This would then lead to the curvature developing at high charge densities in Fig. 7. This is also consistent with the fact that with long times of continuous potential cycling at slow sweep rates, both the A_1 and C_1 peaks decrease in size somewhat, consistent with some residue building up on the electrode surface with time.

Based on the fact that an upper limit to Quat deposition is seen (Fig. 6), this suggests that further Quat reduction is limited by the film thickness and (or) resistance. Even so, for film quantities below 4 mC/cm^2 on GC, there is clearly sufficient conductivity present for film reoxidation to occur, although the large separation of the A_1 and C_1 peaks may also be an indication of the presence of some film resistance.

It is clear that the charge densities observed in these experiments are significantly greater than expected for monolayer coverage. Rahman and Ghosh (15) reported that an unsubstituted pyridine molecule occupies ca. 24 Å^2 on various oxide surfaces, based on the analysis of adsorption data using the Langmuir equation. Assuming that the reduction of the Quat involves a two-electron process (see the following section) and that each Quat molecule occupies a minimum area of 24 Å^2 (expected to be larger than this because of the attached groups (Fig. 1)), this yields 4×10^{14} molecules/cm^2 for a single monolayer of reduced Quat 1 (i.e., 130 μC/cm^2 for a two-electron reaction (19)). Therefore, 4 mC/cm^2 would be equivalent to at least 30 monolayers of the reduced Quat film. In fact, it is likely that the film is much thicker than this, even up to the equivalent of 100 monolayers, allowing for a variety of surface configurations, more open packing, and porosity for ion transport during film growth and oxidation.

To understand what the limitations might be in terms of charge transport through the Quat multilayer, the film morphology was examined using AFM, using a lithographically deposited Pt surface to facilitate the positioning of the AFM tip. Figure 8 shows that the Quat film deposits in the form of clusters, and that at longer deposition times, the clusters grow and coalesce. These images are of two different Quat 4 multilayer samples in air. The sample shown in Fig. 8*a* was prepared by holding at –0.9 V for 10 min in a 0.25 mmol/L Quat 4 solution, while the sample shown in Fig. 8*b* was held at –0.9 V for 60 min. The observed morphology of the Quat multilayer, together with the electrochemistry discussed above and the anticipated poor electronic conductivity of the multilayer (see below), suggests that charge transfer during multilayer formation and oxidative dissolution involves the transfer of the cationic Quat monomer to and (or) from the GC substrate via the pores between the Quat clusters. A more detailed discussion of Quat multilayer formation and removal from Pt is presented elsewhere.[5]

Proposed mechanism of Quat reduction–oxidation

As indicated above, the A_1 and C_1 peaks were observed for all quaternary pyridinium compounds examined electrochemically at the GC electrode, indicating that the redox reaction is associated with the pyridinium ring itself, rather than of any of the functional groups attaching the side chain to the meta-position to the ring or of the chains themselves. Indeed, within the group of Quats studied at GC, Table 1 shows that, when the pyridinium charge is more positive because of the electron-withdrawing nature of the attached groups, the C_1 peak potential is less negative under otherwise identical conditions. These data again demonstrate that the C_1 peak is associated with the reduction of the pyridinium nitrogen of the ring.

Scheme 1 shows a possible mechanism for the reduction of the Quat monomer. Previous workers (15, 20) have suggested a similar mechanism for the reduction of NADH (3–5, 18), which has a very similar structure to that of the Quats studied here. Others (3–5) have proposed a series of possible reaction routes for the reduction of nicotinamide under varying pH conditions. Also, a similar reduction mechanism to that in Scheme 1 for analogous substituted pyridinium compounds, but in aprotic solvents, has been suggested (18, 21). In addition, it has been reported that dialkylcarbamoylpyridinium could be reduced to form 1,4-dihydropyridine in an aqueous solution (22). Further, polypyridinium cations of very high molecular weight (> 30 000 g/mol) have been shown to be reduced in nonaqueous solutions on bismuth by the reduction of the pyridinium ring (23). Interestingly, in a separate paper by the same group, it was shown that monopyridinium and polypyridinium cations can cross-link on the bismuth surface to form dimers after the pyridinium ring has been reduced (24).

This proposed two-electron mechanism shown in Scheme 1 demonstrates that the reduced product can be reoxidized, forming the original structure and hence, that the reaction should be reversible, consistent with our observations. When

[5] J.E. Wong, V.I. Birss, and D.T. Cramb. Article in preparation.

Fig. 8. AFM images of Quat 4 multilayer coated Pt electrode in air (*a*) after holding for 20 min and (*b*) after holding for 60 min at –0.9 V vs. SSCE. The line on the image indicates the location of cross section.

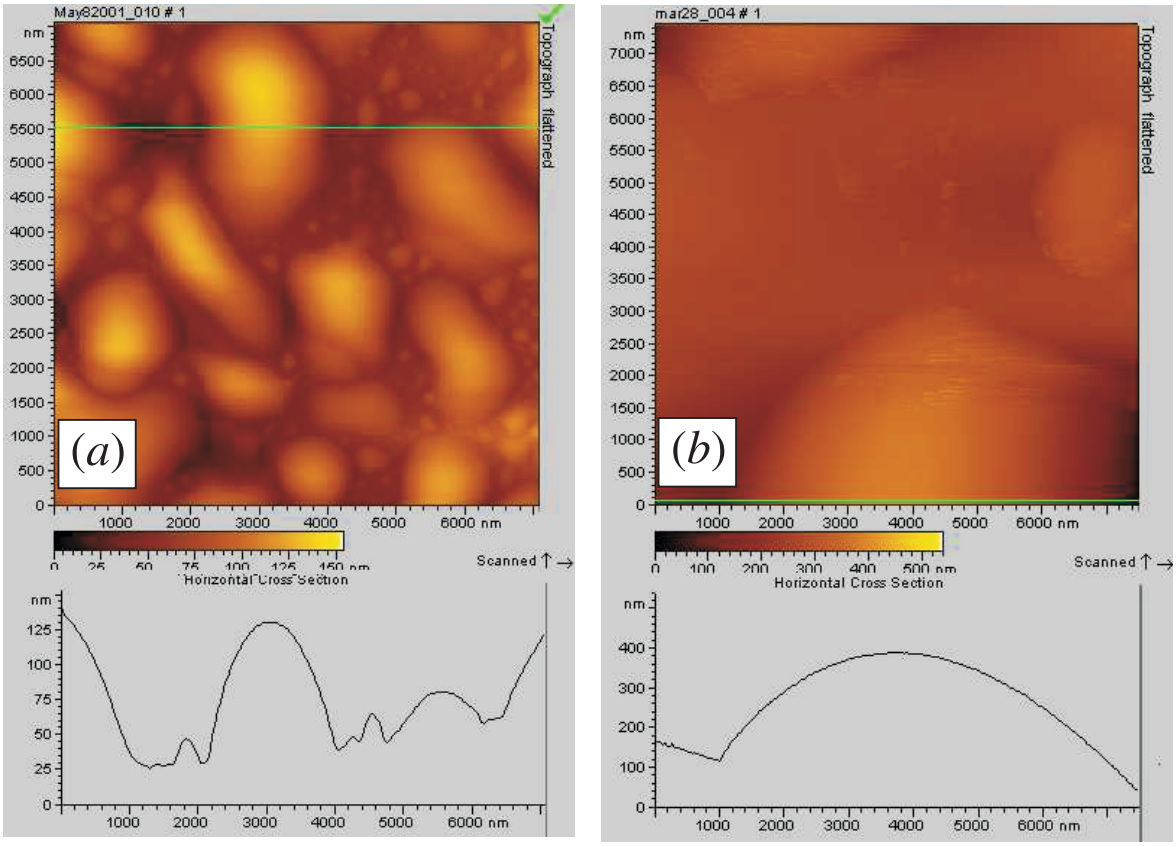

Table 1. Summary of observed peak potentials of Quats 1–3 (1.25 mmol/L Quat in stirred, deaerated pH 7.2 phosphate buffer solution, E_{-} = –1.5 V, E_{+} = 1.0 V, 100 mV/s).

Quat	Reduction peak potential (V)	Oxidation peak potential (V)
1	–1.1	0.1
2	–1.35	–0.2
3	–1.45	–0.55 and –0.1

the Quat is reduced, its positive charge is lost so that a neutral species is generated. This neutral organic molecule would tend to come out of the polar aqueous solution employed in the present work and deposit on the GC electrode surface. When reoxidized, the Quat would regain its positive charge and, therefore, should readily redissolve into the aqueous medium.

Two electrons and one proton are required to reduce the positively charged pyridinium compound to a neutral species, according to this mechanism. This would predict a shift of the reaction redox potential negatively by –29.5 mV per pH unit. It was not possible to test this prediction in this study, as the peak potentials varied with the experimental variables employed, related also to the rate of the concurrent hydrogen evolution reaction on GC.

The radical intermediate suggested in Scheme 1 could potentially initiate the formation of other products. For example, when two of these species react together, a dimer (Scheme 2*a*) could be formed if steric hindrance is not a factor (21). Each dimer would then undergo a two-electron reduction process, not involving protons. However, cleavage of the joining bond in the reoxidation step is not likely and therefore, the reaction in Scheme 2*a* would be irreversible. Instead, a dimeric oxidation product could be formed, as shown in Scheme 2*b*. This redox mechanism would result in an anodic to cathodic charge ratio of two. One electron would be required to form each radical (two electrons per dimer molecule), while four would be required in the oxidation step. As shown in Fig. 7, the charge density in the A_1 and C_1 peaks are very similar, and thus, the formation of this dimeric compound as a primary reaction product is not considered likely in the present case.

After long times of potential cycling, a nonoxidizable residue did seem to build up on the electrode surface, which could be related to the formation of a small amount of the dimeric product. Discrimination between a monomeric vs. dimeric product turned out to be very difficult when GC–MS and NMR analyses were attempted. This is due, in part, to the similarities of the responses of these two products. Also, the ex-situ analysis of this film product was complicated by the possibility of air oxidation of the reduced product once the film-covered electrode was removed from solution.

The radical intermediate shown in Scheme 2*a* could also initiate a nonelectrochemical polymerization process, as depicted in Scheme 3. This polymerization reaction would require the loss of one proton per Quat for its propagation and

Scheme 2. (*a*) Dimerization of two radical intermediate species and (*b*) possible reoxidation of the dimer.

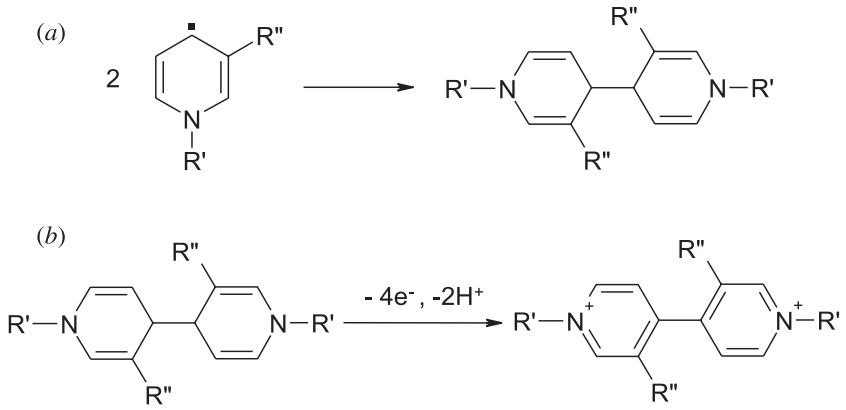

Scheme 3. Possible non-electrochemical polymerization route of a typical Quat.

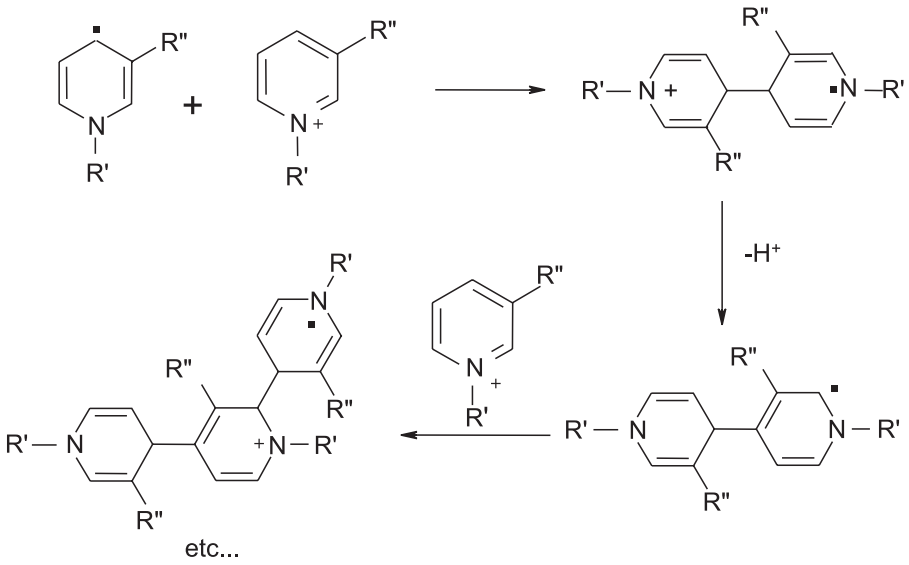

would be expected to occur to a more significant extent in basic solutions, assuming that the OH^- ion will react with the proton to initiate this propagation. Indeed, in exploratory experiments carried out in 0.1 mol/L NaOH solutions, a yellow product was often seen to deposit on the electrode surface (K. Dang, Personal communication, 1998). This may reflect the formation of some polymeric product under these conditions. However, as in the case of the dimeric product, a polymeric product is not likely to be electrochemically oxidizable and is, therefore, inconsistent with the results of Fig. 5. The formation of a polymeric product could potentially explain the slow build-up of nonreactive residue on the GC electrode surface with long times of cycling and as more Quat is deposited (slow sweep rates and long times at E_-).

Summary

In this paper, we have examined the reductive behaviour primarily of *n*-butyl-3-(*N*-octylcarbamyl)pyridinium bromide (Quat 2), but also of *n*-butyl-3-[hydroxy(octylamino)methyl] pyridinium bromide (Quat 1), *n*-benzyl-3,5-dimethyl pyridinium bromide (Quat 3), and *n*-decyl-3-(*N*-hexylcarbamyl) pyridinium bromide (Quat 4) on a glassy carbon (GC) in neutral phosphate buffer solutions. While there is no evidence for the adsorption of the Quats on GC in the normal range of potential, we have demonstrated that all of these Quats can be reduced at potentials more negative that –1.0 V vs. SSCE and that the product deposits as a film on the electrode surface. The corresponding oxidation process, which is seen at ca. –0.2 or –0.3 V, sometimes in two anodic peaks, involves the oxidative dissolution of the film, reforming the original cationic monomer form of the Quat. In general, the amount of Quat that is reduced and deposited is equal to the charge density that passes during its oxidation, although after long times of potential cycling, not all of the surface film can be electrochemically removed.

We have also shown that under the conditions of our experiments, the rate of Quat reduction is likely diffusion controlled, at least initially. At higher Quat concentrations, using slow potential sweep rates, or long times of potential holding, a limit to the amount of Quats that deposits is reached (ca. 4 mC/cm^2), equivalent to ca. 100 monolayers of film. This result, together with the anticipated poor electronic conductivity of the film, argues for a porous film structure. Indeed, AFM studies have shown that the Quat multilayer is composed of clusters, which aggregate together

as more Quat is deposited, thus, ultimately preventing access to the cationic Quat starting material and blocking further multilayer formation.

In terms of the mechanism of Quat reduction, it is shown that the redox chemistry is associated with the pyridinium ring itself, and not with the attached functional groups or side chains. Further, the formation of reduced, neutral monomers is the mostly likely process occurring. Products such as dimers or oligomers may also form, but only after long cycling times, when not all of the Quat reduced can be reoxidized and a residue is observed to build up on the GC electrode surface.

Acknowledgements

We are grateful to the Natural Sciences and Engineering Research Council of Canada (NSERC) Industrial Postgraduate Scholarship program and Brenntag Canada (formerly Travis Chemicals) for the financial support of R.P.C. Wong and J.E. Wong. The authors would also like to thank Dr. Neil Warrender and John Cossar, both formerly of Brenntag Canada, for provision of the Quats and for many helpful discussions. We would also like to acknowledge very useful discussions with Professor Jean Lessard, University of Sherbrooke, in relation to this work.

References

1. V.I. Birss, K. Dang, J.E. Wong, and R.P.C. Wong. J. Electroanal. Chem. **550–551**, 67 (2003).
2. I. Carelli and M.E. Cardinali. J. Electroanal. Chem. **124**, 147 (1981).
3. R.M. Galvin and J.M. Rodriguez-Mellado. J. Electroanal. Chem. **265**, 195 (1989).
4. R.M. Galvin and J.M. Rodriguez-Mellado. J. Electroanal. Chem. **283**, 337 (1990).
5. R.M. Galvin, J.M. Rodriguez-Mellado, and F.G. Blanco. J. Electroanal. Chem. **251**, 163 (1988).
6. X. Ling, J.J. Byerley, M.D. Pritzker, and C.M. Burns. J. Appl. Electrochem. **27**, 1343 (1997).
7. N. Warrender. Travis Chemicals Research Symposium, 1999, Calgary, Alberta.
8. R.P.C. Wong. M.Sc. Thesis, University of Calgary, Calgary, Alberta, 1998.
9. M.M. Ficquelmont-Loizos, H. Takenouti, and W. Kante. J. Electroanal. Chem. **428**, 129 (1997).
10. A.M.O. Brett and F.M. Matysik. J. Electroanal. Chem. **429**, 95 (1997).
11. Robert C. Weast. CRC Handbook of chemistry and physics. 62nd ed. CRC Press, Inc., Boca Raton, Florida. 1981. p. D-126.
12. R.L. McCreery. Carbon electrodes. *In* Electroanalytical chemistry. Vol. 17. *Edited by* A.J. Bard. Marcel Dekker, Inc, New York. 1991.
13. P. Heiduschka, A.W. Munz, and W. Gopel. Electrochim. Acta, **39**, 2207 (1994).
14. Y. Wang, J. Zhang, G. Zhu, and E. Wang. J. Electroanal. Chem. **419**, 1 (1996).
15. M.A. Rahman and A.K. Ghosh. J. Colloid Interface Sci. **77**, 50 (1980).
16. B. Persson. Surface electrochemistry. Plenum, New York. 1993.
17. D.C. Harris. Quantitative chemical analysis. 3rd ed. W.H. Freeman and Company, New York. 1991.
18. J. Volke, L. Dunsch, V. Voleova, A. Petr, and J. Urban. Electrochim. Acta, **42**, 1771 (1997).
19. L. Stolberg, J. Richer, J. Lipkowski, and D.E. Irish. J. Electroanal. Chem. **207**, 213 (1986).
20. S. Sampath and O. Lev. J. Electroanal. Chem. **446**, 57 (1998).
21. J. Volke, J. Urban, and V. Volkeova. Electrochim. Acta, **39**, 13 (1994).
22. J.C. Lepretre, D. Limosin, and G. Pierre. J. Electroanal. Chem. **324**, 115 (1991).
23. G.Y. Vyaseleva, R.K. Sabirov, V.A. Golovin, and M.A. Chizhova. J. Anal. Chem. **49**, 890 (1994).
24. G.Y. Vyaseleva, R.K. Sabirov, I. R. Manyuro, A.E. Gvodeva-Karelina, and V.P. Barabanov. Russ. J. Electrochem. **33**, 126 (1997).